Electric-field-induced intradimer charge disproportionation in the dimer-Mott insulator β^{′}-(BEDT-TTF)_{2}ICl_{2}

Yuma Hattori, Satoshi Iguchi, Takahiko Sasaki, Shinichiro Iwai, Hiromi Taniguchi, and Hideo Kishida

Phys. Rev. B **95**, 085149 — Published 28 February 2017

DOI: 10.1103/PhysRevB.95.085149

Electric-field-induced intradimer charge disproportionation in a dimer-Mott insulator, β'-(BEDT-TTF)$_2$ICl$_2$

Yuma Hattori,[1] Satoshi Iguchi,[2] Takahiko Sasaki,[2] Shinichiro Iwai,[3] Hiromi Taniguchi,[4] and Hideo Kishida[1,*]

[1]Department of Applied Physics, Nagoya University, Nagoya 464-8603, Japan
[2]Institute for Materials Research, Tohoku University, Sendai 980-8577, Japan
[3]Department of Physics, Tohoku University, Sendai 980-8578, Japan
[4]Graduate School of Science and Engineering, Saitama University, Saitama 338-8570, Japan

The Raman scattering spectra of the dimer Mott insulator β'-(BEDT-TTF)$_2$ICl$_2$ [BEDT-TTF = bis(ethylenedithio)tetrathiafulvalene] under a static electric field are investigated. The application of the electric field induces two new Raman peaks on both sides of the original peak position of the charge-sensitive Raman mode (ν_2) in the spectra. At 10 kV/cm, the original peak almost disappears and only the newly emerging peaks are observed. The emergence of new peaks indicates the field-induced charge disproportionation within the dimer. The temporal change of the Raman signals with the inversion of the electric field suggests a macroscopic domain formation of the charge-disproportionate dimers. This picture is reinforced by the direct measurement of the polarization.

PACS: 78.30.Jw, 77.84.Jd

Strong electron correlation effects are key issues in condensed matter physics. They result in many fascinating physical phenomena such as superconductivity, metal-insulator transitions, and various ordering phenomena [1]. Organic molecular compounds based on BEDT-TTF [BEDT-TTF = bis(ethylenedithio)tetrathiafulvalene] molecules afford the opportunity to exploit such strong electron correlation effects and demonstrate novel physical phenomena [2]. Among several intriguing phenomena on strongly correlated systems, the electronic ferroelectricity has been discussed [3-5]. Ferroelectricity is usually the cooperative phenomena of charge displacement and lattice deformation, whereas the electronic ferroelectricity results mainly from electronic displacement and not from lattice deformation [6]. Thus, the electronic ferroelectricity should be essentially characterized by the motion of the electrons accompanied with the emergence of ferroelectricity. Such ferroelectricity often leads to spontaneous and macroscopic electronic displacement, which induces the breakdown of inversion symmetry [3,7].

One of the solutions to achieve this is using charge disproportionation (CD) in dimerized molecular systems. Normally, the ferroelectricity is realized by the deformation of the lattice composed of the positively charged and negatively charged ions, while we can also achieve the ferroelectricity by the charge disproportionation in the modulated or bond-alternated lattice such as dimer systems. Good target materials of the latter strategy are κ-type BEDT-TTF compounds, in which two BEDT-TTF molecules form a dimer and one positive charge is on one dimer unit [2]. When the dimerization is sufficient, the charge is equally distributed in the dimer and the center of the charge is on the gravity center of the dimer. However, when the long-range Coulomb interaction governs the electronic states, the charges favor to be located on the one molecule in a dimer [8-13]. This charge displacement, namely CD, was theoretically proposed in Ref. [14]. The electronic ferroelectricity based on the CD is discussed for κ-(BEDT-TTF)$_2$X compounds experimentally [8-13,15] as well as theoretically [16,17].

For the realization of electronic ferroelectricity, an insulating mechanism is required in the electronic system of the target material. One good example of a highly insulating compound is the β'-(BEDT-TTF)$_2$ICl$_2$ [18], which is an anisotropic quasi-two-dimensional molecular dimer Mott insulator. The ICl$_2$ and BEDT-TTF layers are alternately stacked along the a^* axis ($\perp bc$ plane) [19]. In the crystal, the BEDT-TTF molecules show strong face-to-face dimerization. One electron is transferred from a BEDT-TTF dimer to an ICl$_2$ molecule and the π-orbitals of the BEDT-TTF molecule are +3/4-filled. That is, each dimer has one hole on average. The BEDT-TTF dimers are strongly stacked along the b-axis and form a square lattice [19]. The ICl$_2$ molecules

work as insulating layers, and the transport properties are two-dimensional [20], whereas the band calculation [21] and optical conductivity [22,23] are quasi-one-dimensional. The optical one-dimensionality results from the anisotropy of the transfer integrals; that along the *c*-axis is significantly smaller than that along the *b*-axis in the two-dimensional layer [22,23]. The β'-(BEDT-TTF)$_2$ICl$_2$ shows an antiferromagnetic transition at T_N = 22 K [24,25]. The Heisenberg-model fitting calculation for the temperature dependence of the magnetic susceptibility gives the antiferromagnetic constant $J \approx 59$ K. The ratio of exchange interaction in the *bc*-plane J_b / J_c is ≈ 1.0, which indicates that the magnetic structure is two-dimensional [26].

In this paper, we demonstrate the electric-field-induced CD in β'-(BEDT-TTF)$_2$ICl$_2$, which is revealed by Raman scattering measurements under electric field. In the field-induced state, the valence of each BEDT-TTF molecule is deviated from the average valence and has a specific value. This indicates that part of the charge is transferred from one molecule to another in a BEDT-TTF dimer. The macroscopic slow motion of the charge is also revealed by switching the polarity of the applied electric field. Macroscopic domain formation is supported by polarization measurements as well.

Single crystals of β'-(BEDT-TTF)$_2$ICl$_2$ were grown using an electrochemical method [18,27,28]. The typical dimensions of samples are 200×200×800 μm^3 along the a^*, b', and *c* axes, respectively. The b' axis is defined to be perpendicular to the *c*-axis in the *bc* plane. The electrode spacing was typically 200 μm. We applied the electric field along the b' direction by two electrodes attached on both lateral faces of the crystal. The magnitude of the electric field ranged from 1 kV/cm to 10 kV/cm. An inVia microscopic Raman measurement system (Renishaw) was used for Raman scattering measurements. A conduction-type cryostat (Oxford) was used for low-temperature measurements at 15 K – 300 K. Electric polarization measurements were performed at 10 K, 50 K, and 69 K. In the measurements, we adopted positive-up-negative-down (PUND) methods, by which we can avoid the contribution from the resistance and capacitance components [29,30]. The repetition rate of the measurement was 5 Hz.

Figure 1(a) shows the temperature dependence of the Raman spectra of the (*cc*) polarization configuration for β'-(BEDT-TTF)$_2$ICl$_2$. At 300 K, we observed two peaks at 1469 cm^{-1} and 1494 cm^{-1} and a shoulder structure around 1460 cm^{-1}. With the temperature decrease to values lower than 200 K, the shoulder structure becomes a distinct peak at 1462 cm^{-1}. These three peaks, which are assigned to the C=C stretching modes of BEDT-TTF [31,32] shift to higher frequencies and become sharp with the decrease of temperature. The 1462 cm^{-1} peak was assigned to the ν_{27} C=C stretching

mode, which is Raman-forbidden in an isolated molecule. The dimerization of BEDT-TTF molecules activates this mode in Raman measurements. The other two peaks at 1470 cm^{-1} and 1497 cm^{-1} are respectively assigned to the ν_3 and ν_2 modes of C=C.

To clarify the temperature dependence of the three peaks for the ν_{27}, ν_3, and ν_2 modes, we conducted a fitting analysis using Lorentz functions. As the space group is $P\bar{1}$ and $Z=1$ in β'-(BEDT-TTF)$_2$ICl$_2$ [19], the two vibrational modes in the crystal exist for each molecular ν_{27}, ν_3, and ν_2 mode. These two vibrational modes are divided into a Raman and an infrared active mode. Therefore, each vibrational Raman mode is described by one Lorentz function. On the other hand, the experimentally observed spectral shapes of the ν_3 modes are asymmetrical. In our fitting analysis, we reproduce the ν_3 mode using two Lorentz functions. The peak positions of the stronger mode are adopted in the following analysis. We show the wavenumbers of the peaks for the ν_2 and ν_3 modes in Fig. 1(b). With the decrease of the temperature from 300 K to 15 K, the wavenumbers of the ν_2 and ν_3 modes increase by a few cm^{-1}. Since no anomaly is observed for the spectral shapes with cooling, we conclude that the CD state is not built by lowering the temperature.

Next, we performed the Raman scattering measurement under a static electric field. After cooling to 15 K without electric field (0 kV/cm), we measured the electric field dependence of the Raman spectra in (cc) [Fig. 1(c)] by steps of 1 kV/cm from 0 kV/cm to 5 kV/cm. Between 1 kV/cm and 4 kV/cm, we observed no clear spectral change for the ν_{27}, ν_3, and ν_2 modes. When the electric field intensity was raised to 5 kV/cm, we observed two new peaks at both sides of the ν_2 mode (1492 cm^{-1} and 1510 cm^{-1}). Generally, the frequency of the ν_2 mode simply relates to the valence (ρ) of the BEDT-TTF molecule, which obeys the following relation: $\nu_2(\rho)=1447+120(1-\rho)$ [31,32]. Using this relation, we estimated that the valence of the BEDT-TTF molecule is +0.56 from the frequency of the ν_2 mode at 1500 cm^{-1}. As the formal valence of each dimer is +1, the estimated value (0.56) is reasonable. In a similar way, we evaluated the valence from the wavenumber of the field-induced peaks. The valence of the peaks observed at 1492 cm^{-1} and 1510 cm^{-1} are calculated to be +0.625 and +0.475, respectively. We interpret this result as follows. The valence of one BEDT-TTF molecule in a dimer is +0.475 and that of the other is +0.625 under the electric field. Namely, a +0.075 charge is transferred from one BEDT-TTF to another within a dimer. As a result, the valence of one BEDT-TTF was increased and the valence of the other was decreased. This valence

change suggests that an imbalance in the distribution of electric charge in a dimer, i.e., intradimer CD, occurs.

To further investigate the effect of a high electric field on ν_2 mode, we applied a 10 kV/cm field to another sample. The obtained results are shown in Fig. 1(d). The 1500 cm^{-1} peak is almost suppressed and only the two new peaks are observed, which strongly indicates that the initial states almost disappear and the measured area is perfectly covered with the CD states. The peak positions obtained from the experiments of electric field dependence are shown in Fig. 1(e). It should be noted that the wavenumbers of the peaks do not show any significant dependence on the electric field intensity.

To study the stability of the field-induced states, we measured the Raman spectra under various conditions of applied fields at 15 K. First, we started from the field-induced CD state under 5 kV/cm [(i) in Fig. 2]. Then, we removed the power supply, waited for 30 min, and measured the spectrum with the condition in which the electrodes of the sample are open [open-circuit state, (ii) in Fig. 2]. Then, we shunted the two electrodes, waited for 30 min, and obtained the spectrum [short-circuit state, (iii) in Fig. 2]. Then, we applied an electric field of -5 kV/cm to the sample and measured the spectra [(iv) to (xi) in Fig. 2] every 10 min. The spectra of the states (ii) and (iii) have the side peaks at 1492 cm^{-1} and 1510 cm^{-1}, similarly to the spectrum of the state (i). This strongly indicates that the field-induced CD states can exist without an external field and are essentially stable. We can also claim that such states are a hidden stable state in this material. After the application of the opposite electric field, we observed the quenching of the side peaks at 20 min [(vi) in Fig. 2] and the reappearance of the side peaks at 50 min [(ix) in Fig. 2]. This result makes us imagine that the reversed electric field extinguishes the initial CD state and produces the oppositely directed CD states. The extinction and formation of the CD states by the electric field requires a relatively long period of a few tens of minutes. This indicates that there exists a barrier between non-CD and CD states and that, due to the high resistivity of the sample, the macroscopic charge transfer requires a long time.

To unravel the macroscopic nature of the observed field-induced states, we measured the polarization. In Fig. 3(a), we show the polarization curves measured at 10 K, 50 K, and 69 K. No finite polarizations were observed at 69 K, which is consistent with a previous report [18]. However, at 10 K, finite polarization was observed, whose maximum value reaches 5 nC/cm^2. The sign reversal of the polarization supports the quenching and reappearance of the side peaks of Raman spectra [(v)-(ix) in Fig. 3]. Considering the distance (d) between two BEDT-TTF molecules within a dimer and

assuming that the charge contributing to the induced polarization is $0.15e$, where e is the electron charge, we calculated that the obtained polarization corresponds to around 2.8% of the fully polarized case [33]. This small fraction indicates glassy polarization. In the glassy polarization, the estimated fraction may not correspond to the volume of the crystal but to the surface of the electrodes. Thus, even though we cannot estimate the precise fraction of polar domains, a finite volume of 1% order shows the electric-field-induced CD. Another sample shows polarization curves with two steps at about 19 K [Fig. 3(b)]. This behavior is discussed later.

Here, in order to sketch the physics governing the above experiments, we propose a model as shown in Fig. 4, in which the total energy is plotted versus the position of the charge. In this model, three energy minima are considered as shown in Fig. 4(a). The center valley is the as-prepared state, which is the Mott insulating state. The adjacent two minima are the CD states. This two-minima picture for the CD state is rationalized by the fact that the field-induced state has the two discrete charge values. As mentioned above, the Mott insulating state and the field-induced states coexist in a crystal; thus, two energy pictures are superimposed. Here, there are two possible positions of charge in the field-induced state. In one valley, the charge is located on one side of the two molecules in a dimer. In the other minimum, the charge sits on the other side in the dimer. After the electric field application, the potential surface is slanted and the most stable point moves from the center to the right valley [Fig. 4(b)]. Because there is an energy barrier between the two energy minima, the transition of states requires a certain time as explained in the previous paragraph. After the electric field is off, as shown in the (iii) state of Fig. 2, the energy surface recovers to the initial state. In this state, the potential barrier still exists and the backward transition to the Mott insulating state hardly occurs [Figs. 4(c) and (d)]. When the opposite electric field is applied, the charge moves from the right minimum to the center position and then to the left one. At the center position, the valence of each molecule in a dimer is equivalent. Therefore, in this state, the Raman signal due to the CD disappears. Then, the applied field drives the charge to move to the opposite side that corresponds to the CD state again. The Raman signal due to the CD recovers. This model is also consistent with the polarization curve with two steps in Fig. 3(b), where there are two processes of the electron motion; from the left valley to the central and from the central to the right, and vice versa. If each process occurs in sufficient amount of domains, the two processes correspond to the two steps in the polarization curve.

The model proposed in Fig. 4 describes a macroscopic picture of the observed field-induced CD phenomena. As explained for the time dependence, the CD states

emerge on the minute time scale, which indicates that the formation of the observed CD state is governed by not only a microscopic but also a macroscopic mechanism. For example, the domain formation requires the motion of the domain wall between the CD and Mott states. Naturally, the observed field-induced state is not expected to be spatially homogeneous but to depend on the positions. Actually, no side peaks were observed at some points on the crystal surface even under the electric field. This is a strong evidence of the macroscopic nature of the CD states.

Through the above discussions, we consider that the observed electric-field-induced CD states are the domains consisting of the microscopic dipoles within the dimers. The formation of the observed microscopic states is consistent with the observation of pyroelectricity in this compound reported by Iguchi *et al.* [18]. Both experimental results are obtained under electric field. The microscopic dipoles result in the ferroelectric domains that grow satisfactorily in a macroscopic scale. Such domains should start to show the dynamic nature in the higher temperature, which corresponds to the relaxor-like glassy behaviors observed in Ref. [18].

The present observation is not due to the temporally fluctuating nature of the charge, but to the field-induced static displacement in a dimer. In the field-induced process, the valence does not change continuously from the zero-field state and has a discrete value, which indicates that the electric field creates two new minima in the energy surface. This provides a new strategy to realize the electronic ferroelectricity in the dimer system.

In summary, we clarified the electric-field-induced intradimer CD in β'-(BEDT-TTF)$_2$ICl$_2$ using Raman scattering measurements under static electric fields and polarization measurements by the PUND method. The Raman shifts indicate a transfer of about +/-0.075 valence within a dimer. At high electric fields, the charges are disproportionate for almost all observed sites. The phenomenon includes not only microscopic but also macroscopic mechanisms such as domain formations, which require tens of minutes to emerge. The macroscopic and spatially inhomogeneous domain formation was confirmed in the Raman and polarization measurements. These observations indicate that the hidden stable states are embodied by the applied electric field.

This study was partly supported by JST CREST and JSPS KAKENHI Grant Numbers JP23225005, JP26110512, JP25287080, JP15H02100, JP16K05430, and JP16H00964.

References

* kishida@nuap.nagoya-u.ac.jp

[1] M. Imada, A. Fujimori, and Y. Tokura, Rev. Mod. Phys. **70**, 1039 (1998).

[2] G. Saito and Y. Yoshida, Bull. Chem. Soc. Jpn. **80**, 1 (2007).

[3] K. Yamamoto, S. Iwai, S. Boyko, A. Kashiwazaki, F. Hiramatsu, C. Okabe, N. Nishi, and K. Yakushi, J. Phys. Soc. Jpn. **77**, 074709 (2008).

[4] S. Ishihara, J. Phys. Soc. Jpn. **79**, 011010 (2010).

[5] K. Kobayashi, S. Horiuchi, R. Kumai, F. Kagawa, Y. Murakami, and Y. Tokura, Phys. Rev. Lett. **108**, 237601 (2012).

[6] H. Yamakawa, T. Miyamoto, T. Morimoto, H. Yada, Y. Kinoshita, M. Sotome, N. Kida, K. Yamamoto, K. Iwano, Y. Matsumoto, S. Watanabe, Y. Shimoi, M. Suda, H. M. Yamamoto, H. Mori, and H. Okamoto, Sci. Rep. **6**, 20571 (2016).

[7] H. Itoh, K. Itoh, K. Goto, K. Yamamoto, K. Yakushi, and S. Iwai, Appl. Phys. Lett. **104**, 173302 (2014).

[8] M. Abdel-Jawad, I. Terasaki, T. Sasaki, N. Yoneyama, N. Kobayashi, Y. Uesu, and C. Hotta, Phys. Rev. B **82**, 125119 (2010).

[9] P. Lunkenheimer, J. Müller, S. Krohns, F. Schrettle, A. Loidl, B. Hartmann, R. Rommel, M. de Souza, C. Hotta, J. A. Schlueter, and M. Lang, Nature Mater. **11**, 755 (2012).

[10] K. Itoh, H. Itoh, M. Naka, S. Saito, I. Hosako, N. Yoneyama, S. Ishihara, T. Sasaki, and S. Iwai, Phys. Rev. Lett. **110**, 106401 (2013).

[11] S. Ishihara, J. Phys.: Cond. Mat. **26**, 493201 (2014).

[12] M. Pinterić, M. Čulo, O. Milat, M. Basletić, B. Korin-Hamzić, E. Tafra, A. Hamzić, T. Ivek, T. Peterseim, K. Miyagawa, K. Kanoda, J. A. Schlueter, M. Dressel, and S. Tomić, Phys. Rev. B **90**, 195139 (2014).

[13] M. Pinterić, T.Ivek, M. Čulo, O.Milat, M.Basletić, B.Korin-Hamzić, E.Tafra, A. Hamzić, M. Dressel, and S.Tomić, Physica B **460**, 202 (2015).

[14] H. Seo and H. Fukuyama, J. Phys. Soc. Jpn. **66**, 124 (1997).

[15] K. Sedlmeier, S. Elsässer, D. Neubauer, R. Beyer, D. Wu, T. Ivek, S. Tomić, J. A. Schlueter, and M. Dressel, Phys. Rev. B **86**, 245103 (2012).

[16] C. Hotta, Phys. Rev. B **82**, 241104 (2010).

[17] M. Naka and S. Ishihara, J. Phys. Soc. Jpn. **79**, 063707 (2010).

[18] S. Iguchi, S. Sasaki, N. Yoneyama, H. Taniguchi, T. Nishizaki, and T. Sasaki, Phys. Rev. B **87**, 075107 (2013).

[19] H. Kobayashi, R. Kato, A. Kobayashi, G. Saito, M. Tokumoto, H. Anzai, and T. Ishiguro, Chem. Lett. **15**, 89 (1986).

[20] N. Tajima, R. Kato, and H. Taniguchi, EPL **83**, 27008 (2008).

[21] T. Miyazaki and H. Kino, Phys. Rev. B **68**, 220511(R) (2003).

[22] H. Kuroda, K. Yakushi, H. Tajima, A. Ugawa, M. Tamura, Y. Okawa, A. Kobayashi, R. Kato, H. Kobayashi, and G. Saito, Synth. Met. **27**, A491 (1988).

[23] K. Hashimoto, R. Kobayashi, H. Okamura, H. Taniguchi, Y. Ikemoto, T. Moriwaki, S. Iguchi, M. Naka, S. Ishihara, and T. Sasaki, Phys. Rev. B **92**, 085149 (2015).

[24] M. Tokumoto, H. Anzai, T. Ishiguro, G. Saito, H. Kobayashi, R. Kato, and A. Kobayashi, Synth. Met. **19**, 215 (1987).

[25] N. Yoneyama, A. Miyazaki, T. Enoki, and G. Saito, Synth. Met. **86**, 2029 (1997).

[26] N. Yoneyama, A. Miyazaki, T. Enoki, and G. Saito, Bull. Chem. Soc. Jpn. **72**, 639 (1999).

[27] H. Anzai, M. Tokumoto, T. Ishiguro, G. Saito, H. Kobayashi, R. Kato, and A. Kobayashi, Synth. Met. **19**, 611 (1987).

[28] H. Taniguchi, R. Sato, K. Satoh, A. Kawamoto, H. Okamoto, T. Kobayasi, and K. Mizuno, J. Low. Temp. Phys. **142**, 437 (2006).

[29] J. F. Scott, C. A. Araujo, H. Brett Meadows, L. D. McMillan, and A. Shawabkeh, J. Appl. Phys. **66**, 1444 (1989).

[30] M. Fukunaga and Y. Noda, J. Phys. Soc. Jpn. **77**, 064706 (2008).

[31] H. H. Wang, J. R. Ferraro, J. M. Williams, U. Geiser, and J. A. Schlueter, J. Chem. Soc., Chem. Commun., 1893 (1994).

[32] T. Yamamoto, M. Uruichi, K. Yamamoto, K. Yakushi, A. Kawamoto, and H. Taniguchi, J. Phys. Chem. B **109**, 15226 (2005).

[33] In this calculation, considering that the polarization is the same as the dipole moments perpendicular to the surface per unit volume (V) and the dipole moments are tilted toward the a^* axis by about 19°, the expected full polarization of this system is calculated as $0.075ed\sin19°/V = 178$ nC/cm^2.

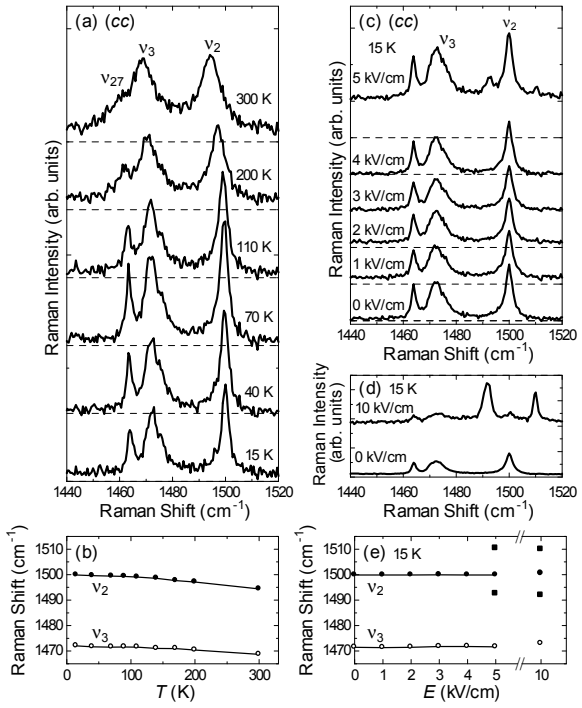

FIG. 1.

(a) Temperature dependence of the Raman spectra in (*cc*) for β'-(BEDT-TTF)$_2$ICl$_2$. Here, (*cc*) denotes that the polarizations of the incident light and the detected light were both set parallel to the *c*-axis. (b) Raman shifts of the ν_2 and ν_3 modes plotted against temperature. (c) Electric-field dependence of the Raman spectra in (*cc*) at 15 K. The electric field (0 – 5 kV/cm) was applied parallel to the b' axis. (d) Raman spectrum at 15 K under 10 kV/cm compared with that without the electric field. (e) Raman shift of the ν_2 and ν_3 modes plotted against applied electric field at 15 K. In (b) and (e), filled and open symbols show the ν_2 and ν_3 modes, respectively. Circles are the original peaks and squares the field-induced peaks.

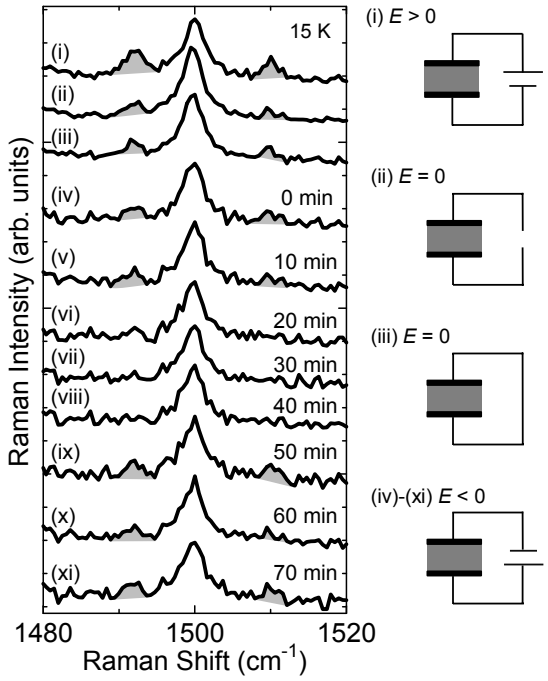

FIG. 2.

Raman spectra of (*cc*) at 15 K and schematics for four experimental configurations. (i): An electric field of 5 kV/cm was applied. (ii): Voltage source was decoupled. (iii): Shunt after (ii). (iv) -(xi): -5 kV/cm was applied.

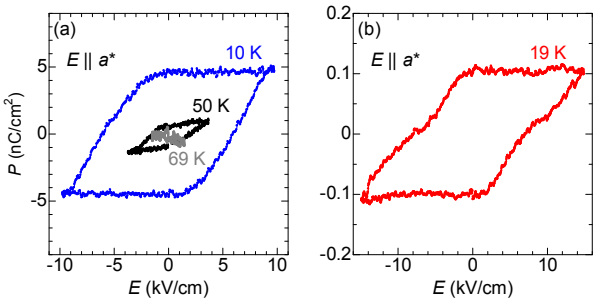

FIG. 3.

Electric field dependence of polarization along the a^* axis measured using the PUND method (a) at 10 K, 50 K, and 69 K and (b) at 19 K for another sample.

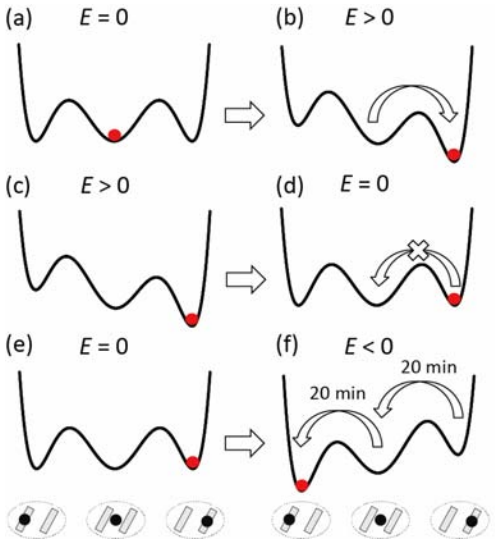

FIG. 4.

Schematics of the three-valley model. The center valley indicates the Mott insulating state, in which the charge is equally distributed to the two constituent BEDT-TTF molecules. The right and left valleys indicate the charge-disproportionate states. The right one corresponds to the state in which the charge is located in the right BEDT-TTF molecule. In the left valley, the charge is located in the left molecule.